Generalized van der Waals equation of state*

William G. Hoover

Department of Applied Science, University of California at Davis–Livermore and Lawrence Livermore Laboratory, Livermore, California 94550

G. Stell, E. Goldmark, and G. D. Degani

State University of New York at Stony Brook, Stony Brook, New York 11790
(Received 18 August 1975)

The quantitative thermodynamic effect of adding a weak, long-range attraction to inverse-power repulsive potentials is studied. The resulting phase diagrams exhibit two fluid phases and a solid phase, a critical point, a triple point, and, for sufficiently soft repulsions, an additional solid phase with an additional triple point. The effects of attractions other than van der Waals' are studied too by using a simple analytic model for the canonical partition function. Although such models exhibit a wide variety of thermodynamic behavior, they are still not general enough to reproduce the results of high-temperature measurements on liquid metals.

I. INTRODUCTION

Van der Waals gave the qualitative explanation of the liquid–gas equilibrium over 100 years ago. Repulsive forces impose a maximum density on the condensed liquid phase, and the attractive forces provide the liquid with a well-defined binding energy. At low temperatures this dense, energetically favored liquid phase can coexist with a much more dilute gas in which entropy compensates for the missing binding energy. The distinction between the liquid and the gas disappears above the *critical temperature*, the lowest temperature at which the thermal energy overcomes the binding energy of the condensed phase.

Van der Waals considered the pressure as a sum of two terms:

$$P = NkT/(V - Nb) - N^2 a/V^2 . \qquad (1)$$

P, V, and T are the pressure (momentum flux), volume, and temperature of the N-particle fluid; k is the Boltzmann constant; Nb represents the volume excluded by the particles' repulsive forces and adds to the flow of momentum; a represents the effect of attractive forces in slowing the momentum flow. The temperature–density phase diagram resulting from the van der Waals equation is shown in Fig. 1.

In the past 20 years extensive use has been made of fast computers[1] in order to obtain and understand the thermodynamic and hydrodynamic properties of model systems with specified simple Hamiltonians. The dominant motivation for this relatively costly work was to augment our understanding of real materials. The greatest success in correlating the computer experiments with real experiments has been achieved with rare gases[2]; progress has also been made in simulating metals[3] and alkali halides.[4] The computer experiments have led to an intuitive appreciation of the physics of melting,[5] the mechanisms of radiation damage[6] and fracture,[7] and hydrodynamic transport processes.[8,9]

In particular, the thermodynamic properties[10–12] for the class of pair potentials,

$$\phi(r) = \epsilon(\sigma/r)^n , \qquad (2)$$

and some of the transport properties[8,9] are now known. The hard-sphere limiting case[10,13] $n = \infty$, is the idealized repulsion van der Waals originally had in mind. Real materials correspond to lower repulsive exponents,[14] with n ranging from about six for metals to about 12 for rare gases. Figure 2 illustrates the variation of pressure with repulsive potential. The figure emphasizes that the thermodynamic properties for very large repulsive exponents ($n \sim \infty$) differ qualitatively from those found for smaller and more realistic values of n. Thus, one way in which the van der Waals model can be generalized is to replace the simple, but crude, hard-sphere model with the more realistic computer results for finite n.[14] Alder and Young have recently
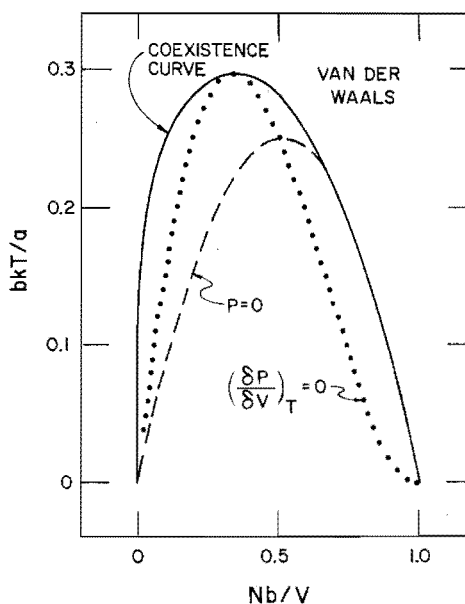
FIG. 1. The van der Waals phase diagram. Within the temperature–density region bounded by the heavy line, the "coexistence curve," two fluid phases with different densities, the gas and the liquid, coexist. Unless the system is permitted to separate into regions of differing density, the equation of state exhibits two different types of macroscopic instability: negative pressure (within the dashed-boundary region) and negative modulus (within the dotted-boundary region).
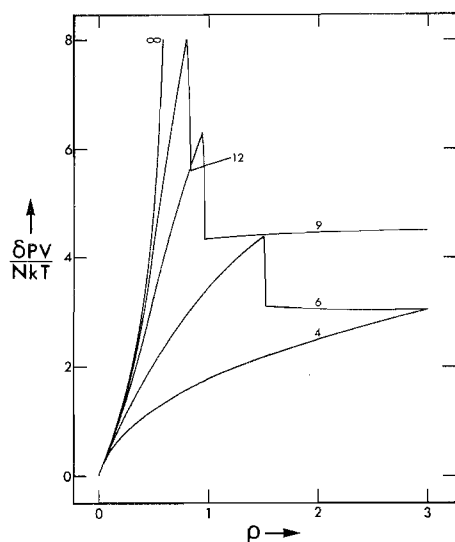
FIG. 2. Excess compressibility factor (relative to that for an ideal gas with the potential energy of a static face-centered cubic solid lattice at the same density) for various inverse power potentials along the isotherm $\epsilon = kT$. The maxima in the $n = 6$, 9, and 12 curves occur at the freezing density. The freezing densities for the $n = 4$ and ∞ cases lie outside the region shown. The variable ρ is $N\sigma^3/(\sqrt{2}V)$.

studied the result of replacing the repulsive part of the van der Waals equation (1) with the correct hard-sphere equation of state.[15] Hiwatari and Matsuda have given a semiquantitative treatment of the effect of adding the van der Waals attraction to the soft-sphere fluid equation of state.[14] We treat this latter problem quantitatively and go beyond the work of Hiwatari and Matsuda to include also the solid-phase properties, including solid–solid equilibriums.

The simple form of the van der Waals attractive term, quadratic in the density, is questionable too. Although this form can be derived rigorously for very-long-range, very-weak potentials,[16] true intermolecular forces are relatively short-ranged, and it is known that electronic contributions to the pressure varying with the $\frac{4}{3}$ and $\frac{5}{3}$ powers of the density are to be expected too.

In this work we first describe the quantitative effect of adding the van der Waals quadratic attractive term to the soft-sphere pressure. We then consider a simple semiquantitative analytic model for the partition function in which the attractive power is varied as well. The results of this model show a wide range of thermodynamic behavior but are still not general enough to describe the experimental data becoming available for liquid metals in the vicinity of the critical point.[17]

II. QUALITATIVE RESULTS

For any system composed of particles interacting with the purely soft-sphere potential, $\epsilon(\sigma/r)^n$, the dimensionless thermodynamic and hydrodynamic properties can be economically expressed in terms of a variable combining the microscopic and macroscopic length and energy scales:

$$x = (N\sigma^3/\sqrt{2}\,V)(\epsilon/kT)^{3/n} . \tag{3}$$

This dimensionless ratio increases monotonically as potential energy increases relative to kinetic energy. For any fixed value of n, two soft-sphere systems with identical values of x share the same equilibrium macroscopic values of PV/NkT, E/NkT (where E is the energy), $\eta(V/N)^{2/3}(mkT)^{-1/2}$ (where η is the shear viscosity and m is the particle mass), and $D(N/V)^{1/3} \times (m/kT)^{1/2}$ (where D is the self-diffusion coefficient). If corresponding dynamical boundary conditions are chosen, the detailed dynamical nonequilibrium histories for two *different* systems with identical values of x (but different densities and temperatures) can be made to coincide. Another way to express the unique simplicity of the soft-sphere system is to point out that only a single isotherm (or isochore or isobar) needs to be studied in order to completely characterize the thermodynamics of the system.

The excess (relative to a static face-centered cubic lattice) compressibility factors for all the cases studied in computer experiments[10-12] appear in Fig. 2. The softest of these ($n = 4$) exhibits a fluid phase and also two different solid phases (body-centered cubic and face-centered cubic).[18] The stiffer case ($n = 12$) has only the close-packed, face-centered phase and the fluid phase.[11] For all of the purely repulsive potentials no gas–liquid equilibrium exists.

How do these simple thermodynamic properties change when an attractive term is added to the potential? Suppose, as van der Waals did, that the effect of the attraction were to decrease the energy per particle by Na/V in the absence of phase separation—where a is the van der Waals a. The corresponding contribution to PV/NkT is

$$-Na/VkT = -\sqrt{2}\,x(a/\epsilon\sigma^3)(\epsilon/kT)^{(n-3)/n} . \tag{4}$$

Because this attractive contribution to the compressibility factor depends separately on x and T, the simple soft-sphere scaling relations are modified. For *any* fixed x, corresponding to either a fluid state or to a solid state for pure soft spheres, the pressure perturbation is always sufficiently great, at low temperatures, to produce negative compressibility factors (and negative pressures). This effect is illustrated, for van der Waals equation, in Fig. 1. Within most of the two-phase coexistence region a homogeneous one-phase system would exhibit both a negative pressure and a negative bulk modulus. Any such state is, of course, thermodynamically unstable relative to a mixed-phase state. The corresponding stable mixed-phase state is a positive-pressure, zero modulus state in which two or three macroscopic phases coexist at different densities. When the phase separation occurs at large x (low temperature) there is a wide density range over which no positive pressures can exist—the two coexisting phases are a solid and a dilute, nearly-ideal gas. If the separation occurs at a smaller x (higher temperature) then two *fluid* phases can be involved, the gas and the liquid. If the temperature is higher still, above the critical temperature, then no unstable region exists and the effect of the attraction is only a small perturbation of the soft-sphere equation of state. Note that the *qualitative* changes in the equation of state, the phase changes, oc-

cur at characteristic values of x alone only in the soft-sphere case. When the attraction is added, these characteristic values depend also on the other dimensionless variable appearing in Eq. (4):

$$(a/\epsilon\sigma^3)(\epsilon/kT)^{1-3/n} .$$

We see that the gross features induced by attraction are (1) an additional fluid phase (the liquid) and (2) characteristic triple-point and critical-point temperatures. It is easy to see too, that in the region of the phase diagram where the perturbation is small, the effect of attraction is to broaden the density gap between coexisting phases. In the next section we study these thermodynamic features quantitatively.

III. QUANTITATIVE RESULTS

In order to make quantitative calculations, we need accurate representations of the soft-sphere reference system solid and fluid phases. For the softest case $n=4$ the fluid-phase computer results[12] are relatively sparse; these, augmented by the lattice-dynamics solid-phase calculations,[18] can be summarized by the following approximate partition functions:

$$z_{fcc} = (kT/\epsilon)^{3/2}(\sigma/\rho\lambda)^3 \exp(-2.8165 - 12.6692x^{4/3}) ,$$

$$z_{bcc} = (kT/\epsilon)^{3/2}(\sigma/\rho\lambda)^3 \exp(-2.7197 - 12.6769x^{4/3}) ,$$

$$z_{fluid} = (\sigma/\lambda)^3\rho^{-1} \exp[+0.616$$
$$-(1.224 + 0.1554\ln x)^5 - 12.6692x^{4/3}] ,$$

(5)

where the lower-case z's indicate Nth roots of N-particle canonical partition functions, $z = e^{-A/NkT}$, where A is the Helmholtz free energy, λ is the de Broglie wavelength, and ρ is $N\sigma^3/(\sqrt{2}V)$.

The phase transitions linking the face-centered, body-centered, and fluid phases correspond to narrow density intervals at $x=6.68$ (where $z_{fcc}=z_{bcc}$) and at $x=3.93$ (where $z_{bcc}=z_{fluid}$). In both cases the density changes by less than a percent across the transition. ($x_{fcc} = 6.677$ and $x_{bcc}=6.676$ for the solid–solid transition; $x_{bcc}=3.94$ and $x_{fluid}=3.92$ for the melting transition.)

It should be noted that the fluid-phase partition function in (5) does not reproduce the known virial form at low density. We justify this logical inconsistency by noting that the radius of convergence of this series must be very small in the inverse fourth power case. Throughout most of the fluid range the energy is dominated by the mean-field lattice sum (proportional to the $\frac{4}{3}$ power of the density).

For the stiffer 12th-power case a more-extensive set of computer investigations[11] has produced the following results:

$$z_{fcc} = (\sigma/\lambda)^3 x^{-6}\rho^{-1} \exp[-6.0659x^4$$
$$-6.3145 - 0.0875x^{-4} + 0.009x^{-8}] ;$$

$$z_{fluid} = (\sigma/\lambda)^3\rho^{-1} \exp[0.65343 - 3.629x$$
$$-3.632x^2 - 3.497x^3 - 2.865x^4 - 0.2176x^{10}] .$$

(6)

These two partition functions are equal at $x=0.82$ and give a two-phase region from $x \doteq 0.805$ to 0.835; the actual fluid–solid transition spans the range from

TABLE I. Phase transition parameters for the inverse 4th-power potential with the van der Waals attraction. The parameters characterizing the coexisting phases, x and y, are defined by Eqs. (3) and (7) of the text. Z is PV/NkT.

Gas–Liquid critical point:	$x=0.194$,	$y=4.03\times10^{-5}$,	$Z=0.307$
Gas–Liquid–bcc triple point:	$x_L=3.85$, $x_B=4.01$,	$y_L=1.83\times10^{-4}$, $y_B=1.91\times10^{-4}$,	$Z_L=0.000$ $Z_B=0.000$
Gas–bcc–fcc triple point:	$x_B=6.67$, $x_F=6.68$,	$y_B=1.99\times10^{-4}$, $y_F=1.99\times10^{-4}$,	$Z_B=0.000$ $Z_F=0.000$

$x = 0.813$ to 0.844.[11]

The effect of adding on a long-range weak van der Waals attraction, the Kac tail,[16] is simply to multiply the pure-phase partition functions just given by $\exp[Na/VkT]$, where the van der Waals a is proportional to the strength of the assumed attraction. Now new features occur in the phase diagrams derived from (5) and (6) with the Kac tail. At characteristic values of x and $(a/\epsilon\sigma^3)(\epsilon/kT)^{(n-3)/n}$ two or three phases can coexist with equal pressures, temperatures, and Gibbs free energies. For any particular choice of a the transition temperature can be determined; then, knowing x, the corresponding density or transition volume can be found for each phase. At each phase transition the combination

$$y = \rho(\epsilon\sigma^3/\sqrt{2}a)^{3/(n-3)}$$

(7)

has a characteristic value for each phase. These numbers appear in Table I for the inverse fourth power repulsion and in Table II for the inverse 12th power repulsion.

We have augmented the 4th- and 12th-power results by using the approximate virial coefficients found by Hutchinson and Conkie[19] to estimate the locations of the gas–liquid critical points for the inverse 6th and 9th power potentials. Several ways of fitting Monte Carlo and integral-equation data suggest uncertainties of 0.002 in PV/NkT and 0.001 in x at the critical point. In the 9th power case we estimated virial coefficients from the graphs given in Ref. 19 and verified that those estimates reproduce PV/NkT within 0.001 at the critical density and temperature. The critical-point parameters, given in Table III, show that the inverse-power repulsive potentials, combined with a van der Waals attraction, all yield critical compressibility factors close to that given by a truncated three-term virial series (for which PV/NkT_c is $\frac{1}{3}$). The densities estimated from such a truncated series are less accurate for the larger

TABLE II. Phase transition parameters for the inverse 12th-power potential with the van der Waals attraction. The parameters characterizing the coexisting phases, x and y, are defined by Eqs. (3) and (7) of the text. Z is PV/NkT.

Gas–Liquid critical point:	$x=0.159$,	$y=0.0761$,	$Z=0.355$
Gas–Liquid–fcc triple point	$x_L=0.785$, $x_F=0.830$,	$y_L=0.277$, $y_F=0.301$,	$Z_L=0.000$ $Z_F=0.000$

TABLE III. Estimated critical parameters for repulsive pair potentials with a van der Waals attraction. The critical values of x, PV/NkT, and the attractive contribution to PV/NkT, are tabulated. In the last column the critical compressibility factor from the approximate model introduced in Sec. IV is given.

n	x	z	Z_a	Z_m
4	0.194	0.307	−3.27	0.381
6	0.165	0.335	−1.85	0.416
9	0.160	0.348	−1.55	0.375[a]
12	0.159	0.355	−1.46	0.315

[a]This value is the same as the van der Waals value because the approximate-model thermal energy is linear in density for the inverse 9th-power potential.

values of repulsive power n.

Because the introduction of the correct repulsive equation of state in the van der Waals equation has little effect, reducing the critical compressibility factor only about half way from van der Waals 0.375 toward the experimental value of 0.29, we have considered the effect of the less-exact but more-flexible models considered in the following section.

IV. SIMPLE MODEL PARTITION FUNCTION

Motivated by the relatively poor compressibility factors resulting from the van der Waals form of the attractive potential, as well as the knowledge that real systems have more complicated density dependences,

FREEZING POINTS
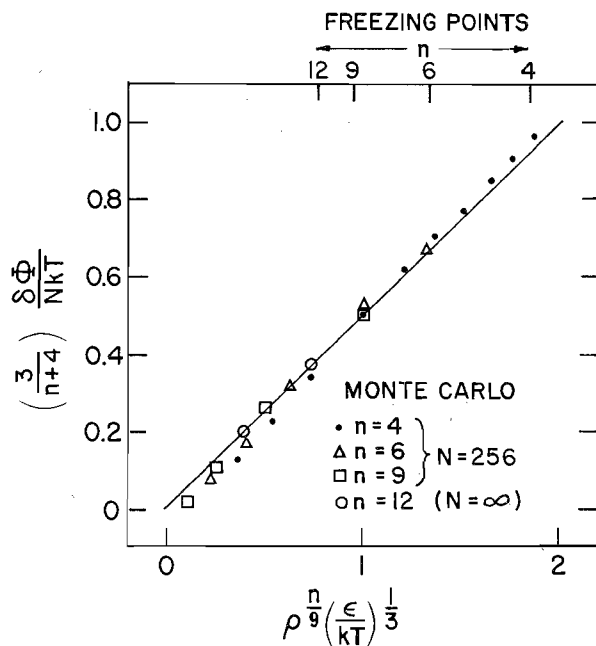
FIG. 3. Comparison of computer-generated results for the thermal potential energy $\delta\Phi$, with the approximation given by Eq. (8) of the text. Although the straight-line approximation is known to fail at low density, where the virial expansion is valid, it is useful for exploratory calculations throughout the fluid portion of the phase diagram. Along the top of the figure the freezing points are indicated for the inverse 4th-, 6th-, 9th-, and 12th-power potentials.
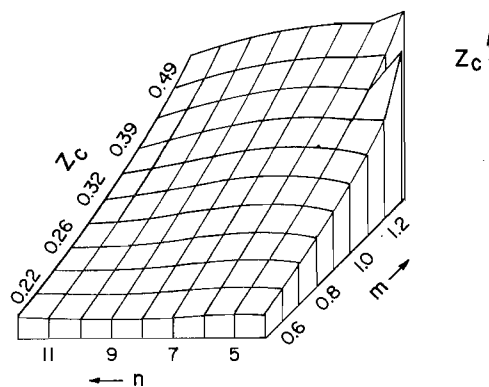
FIG. 4. Compressibility factors at the critical point, $Z_c \equiv PV/NkT_c$, for various combinations of the repulsive exponent n and the attractive exponent m. The traditional van der Waals attraction, linear in density, corresponds to $m=1$.

we explore the generalization of the *attractive* contribution to the thermodynamics. Because the result is only a *model*, not the rigorous consequence of fundamental principles, we are justified in using a crude representation of the repulsive equation of state. For the thermal energy (relative to a static face-centered lattice at the same density) we use

$$\frac{\delta\Phi}{NkT} = \frac{1}{6}(n+4)\rho^{n/9}(\epsilon/kT)^{1/3} . \tag{8}$$

A comparison of this empirical expression with the Monte Carlo data appears in Fig. 3. Recently DeWitt has investigated other, more precise fits to these data.[20]

Our generalization of the van der Waals mean-field attraction, proportional to density, is to chose the attractive potential energy proportional to the mth *power of the density*. Thus the per-particle partition function has the form:

$$z = \frac{Ve}{N\lambda^3} \exp\left[\frac{-\Phi_0}{NkT} - \frac{3\delta\Phi}{NkT} + \frac{a}{kT}\rho^m\right] . \tag{9}$$

This model has actually proved useful in describing experimental results for metals at high temperatures[17] although later unpublished results for tantalum[21] indicate the need for even more flexibility.

Some of the interesting features of this generalized van der Waals partition function are illustrated in Figs. 4 and 5. In Fig. 4 the variation of the critical compressibility factor, PV/NkT_c, with repulsive power n and attractive power m, is shown. Over the reasonably small range of values shown, the critical value varies from 0.1 to 0.7. This enhanced variation shows that the critical point is sensitive to the form of the attractions upon which it depends. This attractive dependence is certainly strong enough to explain the discrepancy of order 0.05 between experiment and the linear van der Waals theory.

In Fig. 5 we have indicated the extent of the liquid range. This can be controlled by varying the magnitude of the van der Waals a and the calculations were carried out as follows: The two conditions $P=0$ and E/NkT
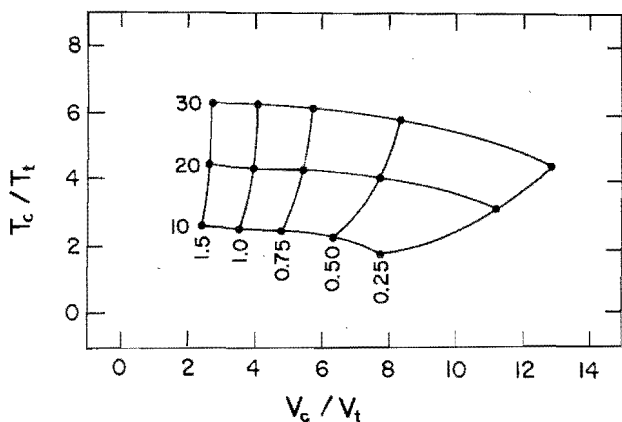
FIG. 5. Variation of the extent of the liquid range, T_c/T_t and V_c/V_t, with strength of the attractive exponent m and reduced binding energy E/NkT assuming an inverse 12th-power repulsion. Similar results are obtained for other values of n. In the figure the results for $m = 0.25$ to 1.5, with E/NkT varying from 10 to 30, are shown.

= const give two conditions on the zero-pressure density and temperature. These can then be combined with the two critical-point conditions on density and temperature to calculate the ratios T_c/T_t and V_c/V_t, where T_t and V_t are taken, with negligible error, to be the zero-pressure state at which the energy is fixed. Because, as with the critical compressibility factor, the results are more sensitive to m than to n, we show in Fig. 5 the variation of the temperature and volume ratios only for the inverse 12th-power repulsion. As expected, the extent of the liquid range is enhanced by increasing the binding energy relative to kT_t. Experimental values of this binding energy vary from about 10 to 40 times kT_t.

Although the present model is still not flexible enough to describe the electronic effects present in real liquid metals in complete detail, we believe that it does represent a useful basis from which to construct quantitative representations of experimental data required for calculations with real materials.

V. ACKNOWLEDGMENTS

[*]This work was supported by the United States Atomic Energy Commission and by its successor, the Energy Research and Development Administration.

[1]See, for instance, the review by W. W. Wood, in *Physics of Simple Liquids*, edited by H. N. V. Temperley, J. S. Rowlinson, and G. S. Rushbrooke (North-Holland, Amsterdam, 1968), Chap. 5.

[2]J. A. Barker, M. V. Bobetic, and A. Pompe, Mol. Phys. 20, 347 (1971).

[3]N. W. Ashcroft and J. Lekner, Phys. Rev. 145, 83 (1966); H. Jones, J. Chem. Phys. 55, 2640 (1971).

[4]F. H. Ree and A. Holt, Phys. Rev. B 8, 826 (1973).

[5]W. G. Hoover and M. Ross, Contemp. Phys. 12, 339 (1971).

[6]G. H. Vineyard in *Interatomic Potentials and Simulation of Lattice Defects*, edited by P. C. Gehlen, J. R. Beeler, and R. I. Jaffee (Plenum, New York, 1972), p. 3.

[7]W. G. Hoover, W. T. Ashurst, and R. Cook, in *Proc. Fifth Atlas Computer Symposium* (Oxford University, April 1975, in press).

[8]W. T. Ashurst, Ph.D. dissertation, University of California at Davis-Livermore 1974; W. T. Ashurst and W. G. Hoover, Phys. Rev. A 11, 658 (1975); D. Levesque, L. Verlet, and J. Kurkijarvi, Phys. Rev. A 7, 1690 (1973).

[9]M. Ross and P. Schofield, J. Phys. C 4, L305 (1973).

[10]For $n = \infty$ see B. J. Alder, W. G. Hoover, and D. A. Young, J. Chem. Phys. 49, 3688 and W. G. Hoover and F. H. Ree, J. Chem. Phys. 49, 3609 (1968).

[11]For $n = 12$ see W. G. Hoover, M. Ross, K. W. Johnson, D. Henderson, J. A. Barker, and B. C. Brown, J. Chem. Phys 52, 4931 (1970) and J. P. Hansen, Phys. Rev. A 2, 221 (1970).

[12]For smaller n see W. G. Hoover, S. G. Gray, and K. W. Johnson, J. Chem. Phys. 55, 1128 (1971) as well as Ref. 19.

[13]A useful hard-sphere fluid equation of state is given by N. F. Carnahan and K. E. Starling, J. Chem. Phys. 51, 635 (1969).

[14]H. Matsuda and Y. Hiwatari, Prog. Theor. Phys. 47, 741 (1972) and in *Cooperative Phenomena*, edited by H. Haken and M. Wagner (Springer-Verlag, Berlin, 1973), p. 249.

[15]D. A. Young and B. J. Alder, Phys. Rev. A 3, 364 (1971).

[16]See, for example, J. L. Lebowtiz and O. Penrose, J. Math. Phys. 5, 841 (1964).

[17]G. R. Gathers, J. W. Shaner, and D. A. Young, Phys. Rev. Lett. 33, 70 (1974).

[18]W. G. Hoover, D. A. Young, and R. Grover, J. Chem. Phys. 56, 2207 (1972).

[19]P. Hutchinson and W. R. Conkie, Mol. Phys. 21, 881 (1971); 24, 567 (1972).

[20]H. DeWitt (private communication).

[21]J. Shaner, G. R. Gathers, D. A. Young, and C. Minichino (submitted to High Temp.—High Pressures).